Journal of Solid State Chemistry **166,** 164–170 (2002)
doi:10.1006/jssc.2002.9575, available online at http://www.idealibrary.com on IDEAL®

High-Pressure Synthesis and Crystal Structure of B_2S_3

Takeshi Sasaki, Hirotsugu Takizawa,[1] Kyota Uheda, Takahiro Yamashita, and Tadashi Endo

Department of Materials Chemistry, Graduate School of Engineering, Tohoku University, Aoba-yama 07, Sendai 980-8579, Japan

Received November 26, 2001; in revised form February 12, 2002; accepted March 1, 2002

Two new high-pressure phases of binary boron–sulfur compounds, B_2S_3-II and B_2S_3-III, were synthesized at 3–6.2 GPa. A single crystal of B_2S_3-III was grown and the structure was determined (tetragonal, space group $I4_1/a$, $a = 16.086(2)$ Å, $c = 30.488(4)$ Å; $V = 7888(1)$ Å^3, $Z = 100$, $R = 3.0\%$ and $R_w = 2.8\%$ for 3047 observed data [$I > 3.00\sigma(I)$]. The structure of B_2S_3-III consists of two kinds of macrotetrahedra built up from 20 and 34 BS_4-tetrahedra. These macrotetrahedra connect each other to form an interpenetrating zincblende-type structure by sharing BS_4-tetrahedra at the corners of those. B_2S_3-III is anticipated having a rather disordered structure. From the UV-Vis diffuse reflectance spectrum, the optical band gap of B_2S_3-III was estimated to be 3.7 eV. © 2002 Elsevier Science (USA)

Key Words: **boron sulfide; high pressure; crystal structure; macrotetrahedron.**

INTRODUCTION

Binary boron–sulfur compounds (boron sulfides), $B_{12}S$ (1), B_2S_3 (2), $(BS_2)_n$ [3,4) and B_8S_{16} [4], are known to exhibit characteristic crystal structures. Although $B_{12}S$ has the α-rhombohedral-boron-type structure (1), other compounds are made up of planar BS_3 triangles composed of sp^2-hybridized trigonal boron atoms. The crystal chemistry of the boron–sulfur system has been precisely reviewed by Krebs *et al.* (5, 6).

The above-mentioned binary compounds are synthesized at ambient pressure condition and have crystal structures with rather low atomic packing density. It is expected that new compounds having dense-packed structures with sp^3-hybridized tetrahedral boron atoms would be synthesized under high pressure, however, those have not been studied well except for (boron monosulfide) (BS). Boron monosulfide was synthesized in two modifications at ca. 6 GPa (7). The one is an orthorhombic phase (*o*-BS) obtained at 1400°C, and the other is a cubic phase (*c*-BS) obtained above 1500°C. But crystal structures of both phases have not been determined yet.

In our previous study, high-pressure synthesis in this system was performed and the existence of rhombohedral boron monosulfide (*r*-BS) with a GaS 3R-type structure was confirmed by the X-ray diffraction analysis (8). But so far, the crystal structures have not been determined completely. In this paper, two new stoichiometric high-pressure forms of binary B–S compounds, named B_2S_3-II and B_2S_3-III, are reported and the crystal structure of B_2S_3-III determined by the single-crystal X-ray diffraction data is described.

EXPERIMENTAL

High-Pressure Synthesis

Powders of elemental amorphous boron (4N) and crystalline orthorhombic sulfur (4N) were used as starting materials. The mixed powder was pressed into a small pellet and placed in a cylindrical boron nitride capsule. Then, the sealed capsule was inserted into the cell assemblage which was composed of NaCl sleeves and a carbon heater. The reactions were carried out within the pressure range 3–6.2 GPa using a belt-type high-pressure equipment. The reaction temperature and duration were 400–1600°C and 30 min. After the high-pressure/temperature reaction, the sample was quenched to room temperature before the release of the applied pressure.

The obtained sample was analyzed by a Rigaku RINT2000 X-ray diffractometer using graphite-monochromated Cu*K*α radiation. UV-Vis diffuse reflectance spectra were measured by a JASCO V-570 UV-Vis spectrophotometer. The chemical composition was analyzed by X-ray photoelectron spectroscopy (ESCA, Shimadzu ESCA-750).

Single Crystal Structure Determination

A transparent pale-yellow crystal of B_2S_3-III having approximate dimensions of $0.3 \times 0.2 \times 0.2$ mm^3 was obtained. The X-ray diffraction intensity data were collected with a four circle diffractometer Rigaku AFC7R using graphite-monochromated Mo*K*α radiation and a rotating anode generator. The crystallographic data are summarized in

---

[1] To whom correspondence should be addressed. Fax: + 81-22-217-7228. E-mail: takizawa@aim.che.tohoku.ac.jp.

0022-4596/02 $35.00

TABLE 1
Crystallographic Data for B_2S_3-III

Empirical formula	B_2S_3
Formula weight	117.80
Diffractometer type	Rigaku AFC7R
Monochromator	Graphite
Scan type	ω–2θ
Temperature	23.0°C
Wavelength	0.71069 Å (Mo$K\alpha$)
Crystal system	Tetragonal
Space group	$I4_1/a$
Unit cell dimensions	$a = 16.086(2)$ Å $c = 30.488(4)$ Å
Volume	7888(1) $Å^3$
Z	100
Density(calculated)	2.479 g/cm^3
Absorption coefficient	20.39 cm^{-1}
$F(000)$	5800
Crystal size	$0.30 \times 0.20 \times 0.20$ mm^3
$2\theta_{max}$	55.0°
Reflections collected	4969
Independent reflections	4630 ($R_{int} = 0.068$)
Refinement method	Full-matrix least-squares
Data [$I > 3.00\sigma(I)$]	3047
Parameters	283
Goodness of fit	2.09
P-factor	0.001
Residuals: R; R_w	0.030; 0.028
Max. shift/error in final cycle	0.04
Max. peak in final diff.map	$0.68e^-/Å^3$
Min. peak in final diff.map	$-1.18e^-/Å^3$

Note. $R = \sum||F_o| - |F_c||/F_o|$, $R_w = [\sum w(|F_o| - |F_c|)^2/\sum wF_o^2]^{1/2}$, $w = [\sigma_c(F_o)^2 + (PF_o)^2/4]^{-1}$, $\sigma_c(F_o)$ = e.s.d. based on counting statistics, P = P-factor.

Table 1. Cell parameters for data collection, which were obtained from a least-squares refinement using 25 well-centered reflections in the range $29.44 < 2\theta < 30.00°$, corresponded to a tetragonal unit cell with dimensions: $a = 16.086(2)$ Å, $c = 30.488(4)$ Å and $V = 7888(1)$ $Å^3$. The intensity data were collected at a temperature of 23±1°C using the ω–2θ scan technique. The weak reflections [$I < 10.0\sigma(I)$] were rescanned (maximum of five scans) and the counts were accumulated to ensure good counting statistics. An empirical absorption correction based on ψ-scans of several reflections was applied, which resulted in transmission factors ranging from 0.86 to 1.00 and further data were corrected for Lorentz and polarization effects. Of the 4969 reflections collected, 4630 were unique ($R_{int} = 0.068$).

Based on the systematic absences of hkl: $h + k + l \neq 2n$, $hk0$: $h \neq 2n$, $00l$: $l \neq 4n$ and the successful solution and refinement of the structure, the space group was determined to be $I4_1/a$ (#88).

The structure was solved by direct methods using the SIR92 program (9). The final cycle of full-matrix least-squares refinement was based on 3047 observed reflections [$I > 3.00\sigma(I)$] and 283 variable parameters and converged with R indices of: $R = 0.030$, $R_w = 0.028$. All calculations were performed using the teXsan (10) crystallographic software package of Molecular Structure Corporation.

Table 2 gives a list of the final refined atom coordinates. Tables 3 and 4 give lists of distances and angles between boron and sulfur atoms, respectively. Figure 1 shows coordination of atoms in a ball and stick mode.

RESULTS AND DISCUSSION

Synthesis and Phase Identification

In the high-pressure synthesis of binary B–S compounds, relation between reaction condition and product is very complicated. We have so far confirmed the existences of high-pressure phases in this system; *r*-BS [it had been called *o*-BS (7), but in fact, it could be assigned to a rhombohedral unit cell (8)], B_2S_3-II and B_2S_3-III. The existence of compounds having chemical composition of B:S = 2:3 was con-

TABLE 2
Final Atom Parameters for B_2S_3-III
(Standard Deviations Are in Parentheses)

Atom	Position	x	y	z	B_{eq} ($Å^2$)
S(1)	16*f*	0.64079(6)	– 0.12536(6)	– 0.27088(3)	0.43(2)
S(2)	16*f*	0.66481(6)	– 0.00552(6)	– 0.34126(3)	0.45(2)
S(3)	16*f*	0.55721(6)	– 0.16621(6)	– 0.48397(3)	0.43(2)
S(4)	8*e*	0.5000	– 0.2500	– 0.26995(5)	0.69(2)
S(5)	16*f*	0.73475(6)	– 0.40841(6)	– 0.55616(3)	0.41(2)
S(6)	16*f*	0.69045(6)	– 0.14803(6)	– 0.26493(3)	0.44(2)
S(7)	16*f*	0.64787(6)	– 0.11918	– 0.12314(3)	0.50(2)
S(8)	16*f*	0.69059(6)	– 0.13914(6)	– 0.41205(3)	0.43(2)
S(9)	16*f*	0.51757(6)	– 0.02528(6)	– 0.12313(4)	0.67(2)
S(10)	16*f*	0.82474(6	– 0.11945(6)	– 0.33833(3)	0.60(2)
S(11)	16*f*	0.63781(6)	– 0.26194(6)	– 0.19904(3)	0.48(2)
S(12)	16*f*	0.49983(6)	– 0.10028(6)	– 0.34059(3)	0.64(2)
S(13)	16*f*	0.78122(6)	– 0.13653(6)	– 0.19762(3)	0.59(2)
S(14)	4*b*	0.5000	– 0.2500	– 0.1250	1.16(2)
S(15)	16*f*	0.71682(6)	– 0.28057(6)	– 0.33696(3)	0.44(2)
S(16)	16*f*	0.50362(6)	– 0.11037(6)	– 0.19727(3)	0.45(2)
S(17)	16*f*	0.71602(6)	– 0.27088(6)	– 0.48394(3)	0.43(2)
S(18)	16*f*	0.42356(6)	– 0.19725(6)	– 0.55599(3)	0.60(2)
S(19)	16*f*	0.79804(6)	0.00902(6)	– 0.26714(3)	0.56(2)
S(20)	16f	0.55278(6)	– 0.17081(6)	– 0.33984(4)	0.40(2)
B(1)	16*f*	0.5771(3)	0.0439(3)	– 0.3057(2)	0.60(3)
B(2)	16*f*	0.5667(3)	– 0.1879(3)	– 0.2327(1)	0.54(8)
B(3)	16*f*	0.7175(3)	0.0634(3)	– 0.2325(2)	0.59(8)
B(4)	16*f*	0.7706(3)	– 0.1965(3)	– 0.3740(2)	0.66(8)
B(5)	16*f*	0.4349(3)	0.1780(3)	– 0.1608(2)	1.02(9)
B(6)	16*f*	0.6549(3)	– 0.3511(3)	– 0.5189(2)	0.52(8)
B(7)	16*f*	0.5770(3)	0.0483(3)	– 0.1587(2)	0.70(8)
B(8)	16*f*	0.7082(3)	0.1960(3)	– 0.1614(1)	0.57(8)
B(9)	16*f*	0.6080(3)	– 0.0887(3)	– 0.3747(1)	0.47(7)
B(10)	8*e*	0.5000	– 0.2500	– 0.5198(2)	0.6(1)
B(11)	16*f*	0.7429(3)	– 0.0670(3)	– 0.3038(1)	0.55(8)
B(12)	16*f*	0.6331(3)	– 0.2238(3)	– 0.3026(2)	0.51(8)
B(13)	16*f*	0.6345(3)	– 0.2229(3)	– 0.4463(1)	0.50(8)

TABLE 3
Interatomic Distances (Å) (Standard Deviations Are in Parentheses)

Atoms	Distance	Atoms	Distance	Atoms	Distance
B(1)–S(1)	1.973(4)	B(11)–S(2)	1.965(4)	S(9)–B(7)	1.868(5)
S(2)	1.949(5)	S(6)	1.952(4)	B(8)	1.898(4)
S(12)	1.871(4)	S(10)	1.887(5)		
S(17)	1.961(5)	S(19)	1.878(4)	S(10)–B(4)	1.865(5)
B(2)–S(1)	1.944(4)	B(12)–S(3)	1.917(4)	B(11)	1.887(5)
S(4)	1.854(4)	S(6)	1.912(5)	S(1)–B(2)	1.945(5)
S(11)	1.945(5)	S(15)	1.935(5)	B(5)	1.913(5)
S(16)	1.937(4)	S(20)	1.920(4)	B(8)	1.930(4)
B(3)–S(1)	1.971(5)	B(13)–S(3)	1.922(4)	S(12)–B(1)	1.871(4)
S(5)	1.972(5)	S(8)	1.930(4)	B(4)	1.883(5)
S(13)	1.888(4)	S(17)	1.905(4)		
S(19)	1.888(4)	S(20)	1.913(4)	S(13)–B(3)	1.888(4)
				B(8)	1.875(4)
B(4)–S(8)	1.963(5)				
S(10)	1.865(5)			S(14)–B(5)	1.906(6)
S(12)	1.883(5)			B(5)′	1.906(6)
S(15)	1.962(5)	S(1)–B(1)	1.973(4)	B(5)″	1.906(6)
		B(2)	1.944(4)	B(5)‴	1.906(6)
B(5)–S(7)	1.918(5)	B(3)	1.971(5)		
S(11)	1.913(5)			S(15)–B(4)	1.962(5)
S(14)	1.906(6)	S(2)–B(1)	1.949(5)	B(9)	1.928(4)
S(16)	1.908(5)	B(9)	1.915(4)	B(12)	1.935(5)
		B(11)	1.965(4)		
B(6)–S(5)	1.946(4)			S(16)–B(2)	1.937(4)
S(6)	1.963(4)	S(3)–B(10)	1.964(4)	B(5)	1.908(5)
S(17)	1.942(4)	B(12)	1.917(4)	B(7)	1.943(5)
S(18)	1.865(5)	B(13)	1.922(4)		
				S(17)–B(1)	1.961(5)
B(7)–S(5)	1.977(5)	S(4)–B(2)	1.854(4)	B(6)	1.942(4)
S(7)	1.943(5)	B(2)′	1.854(4)	B(13)	1.905(4)
S(9)	1.868(5)				
S(16)	1.943(5)	S(5)–B(3)	1.972(5)	S(18)–B(6)	1.865(5)
		B(6)	1.946(4)	B(10)	1.858(4)
B(8)–S(7)	1.956(4)	B(7)	1.977(5)		
S(9)	1.898(4)			S(19)–B(3)	1.888(4)
S(11)	1.930(4)	S(6)–B(6)	1.963(4)	B(11)	1.878(4)
S(13)	1.875(4)	B(11)	1.952(4)		
		B(12)	1.912(5)	S(20)–B(9)	1.913(4)
B(9)–S(2)	1.915(4)			B(12)	1.920(4)
S(8)	1.928(5)	S(7)–B(5)	1.918(5)	B(13)	1.913(4)
S(15)	1.928(4)	B(7)	1.943(5)		
S(20)	1.913(4)	B(8)	1.956(4)		
B(10)–S(3)	1.964(4)	S(8)–B(4)	1.963(5)		
S(3)′	1.964(4)	B(9)	1.928(5)		
S(18)	1.858(4)	B(13)	1.930(4)		
S(18)′	1.858(4)				

firmed by experiments varying the nominal compositions of the starting materials. When the nominal composition deviated from 2:3, the product contained excess unreacted material or other by-products. The reaction conditions for the synthesis of these phases were examined by varying the reaction temperature and pressure. According to the chemical analysis, the obtained materials consist of only boron and sulfur, though the atomic ratios have not been determined credibly due to sublimation of surface atoms.

Figure 2 shows the P–T diagram for the syntheses of B_2S_3-II and B_2S_3-III studied in the range of 3–6.2 GPa and 400–1600°C at the fixed nominal composition of $B:S = 2:3$. As shown in the figure, boron and sulfur do not react with each other below 400°C. Above 500°C, the product depends on the pressure condition. At 3 GPa, a partial reaction

TABLE 4
Bond Angles [deg] (Standard Deviations Are in Parentheses)

Atoms	Angle	Atoms	Angle
S(1)–B(1)–S(2)	101.2(2)	S(7)–B(8)–S(9)	109.5(2)
S(1)–B(1)–S(12)	109.2(2)	S(7)–B(8)–S(11)	114.3(2)
S(1)–B(1)–S(17)	109.4(2)	S(7)–B(8)–S(13)	109.9(2)
S(2)–B(1)–S(12)	111.2(2)	S(9)–B(8)–S(11)	109.3(2)
S(2)–B(1)–S(17)	114.6(2)	S(9)–B(8)–S(13)	106.2(2)
S(12)–B(1)–S(17)	110.7(2)	S(11)–B(8)–S(13)	107.3(2)
S(1)–B(2)–S(4)	105.5(2)	S(2)–B(9)–S(8)	106.2(2)
S(1)–(B(2)–S(11)	105.8(2)	S(2)–B(9)–S(15)	107.9(2)
S(1)–B(2)–S(16)	108.8(2)	S(2)–B(9)–S(20)	114.1(2)
S(4)–B(2)–S(11)	109.5(2)	S(8)–B(9)–S(15)	106.4(2)
S(4)–B(2)–S(16)	112.6(2)	S(8)–B(9)–S(20)	111.0(2)
S(11)–B(2)–S(16)	114.0(2)	S(15)–B(9)–S(20)	110.9(2)
S(1)–B(3)–S(5)	112.2(2)	S(3)–B(10)–S(3)′	112.4(3)
S(1)–B(3)–S(13)	111.1(2)	S(3)–B(10)–S(18)′	109.09(4)
S(1)–B(3)–S(19)	109.3(2)	S(3)–B(10)–S(18)′	109.50(4)
S(5)–B(3)–S(13)	109.0(2)	S(3)′–B(10)(–S(18)	109.50(4)
S(5)–B(3)–S(19)	111.6(2)	S(3)′–B(10)–S(18)′	109.09(4)
S(13)–B(3)–S(19)	103.4(2)	S(18)–B(10)–S(18)′	107.1(3)
S(8)–B(4)–S(10)	109.8(2)	S(2)–B(11)–S(6)	114.4(2)
S(8)–B(4)–S(12)	108.8(2)	S(2)–B(11)–S(10)	110.2(2)
S(8)–B(4)–S(15)	112.0(2)	S(2)–B(11)–S(19)	108.7(2)
S(10)–B(4)–S(12)	108.6(2)	S(6)–B(11)–S(10)	110.0(2)
S(10)–B(4)–S(15)	109.2(2)	S(6)–B(11)–S(19)	106.2(2)
S(12)–B(4)–S(15)	108.4(2)	S(10)–B(11)–S(19)	107.1(2)
S(7)–B(5)–S(11)	108.3(2)	S(3)–B(12)–S(6)	107.2(2)
S(7)–B(5)–S(14)	112.3(3)	S(3)–B(12)–S(15)	105.8(2)
S(7)–B(5)–S(16)	105.8(2)	S(3)–B(12)–S(20)	112.1(2)
S(11)–B(5)–S(14)	112.2(2)	S(6)–B12–S(15)	106.9(2)
S(11)–B(5)–S(16)	106.7(3)	S(6)–B(12)–S(20)	113.4(2)
S(14)–B(5)–S(16)	111.2(2)	S(15)–B(12)–S(20)	111.0(2)
S(5)–B(6)–S(6)	104.3(2)	S(3)–B(13)–S(8)	107.1(2)
S(5)–B(6)–S(17)	107.5(2)	S(3)–B(13)–S(17)	106.2(2)
S(5)–B(6)–S(18)	106.9(2)	S(3)–B(13)–S(20)	111.2(2)
S(6)–B(6)–S(17)	114.7(2)	S(8)–B(13)–S(17)	106.7(2)
S(6)–B(6)–S(18)	109.3(2)	S(8)–B(13)–S(20)	112.0(2)
S(17)–B(6)–S(18)	113.5(2)	S(17)–B(13)–S(20)	113.3(2)
S(5)–B(7)–S(7)	102.5(2)		
S(5)–B(7)–S(9)	109.0(2)		
S(5)–B(7)–S(16)	109.9(2)		
S(7)–B(7)–S(9)	110.4(2)		
S(7)–B(7)–S(16)	113.1(2)		
S(9)–B(7)–S(16)	111.5(2)		

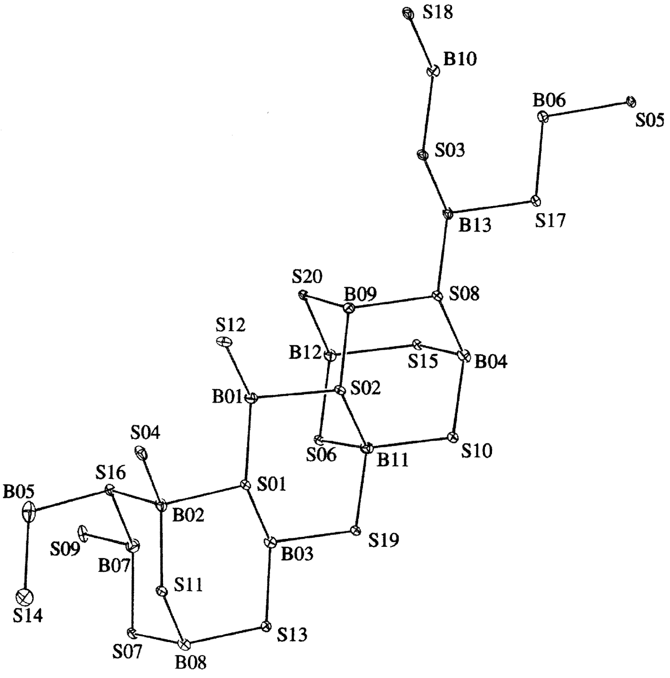

FIG. 1. Atom coordinates in B_2S_3-III showing thermal ellipsoids.

occurred and BS_2, which can be formed at ambient pressure, was obtained at 500°C prior to the formation of B_2S_3-II above 600°C. However, above 5 GPa, no reaction occurred at 500°C. At 600°C, a reaction took place and an amorphous phase was formed, then it crystallized into B_2S_3-II having white color above 800°C.

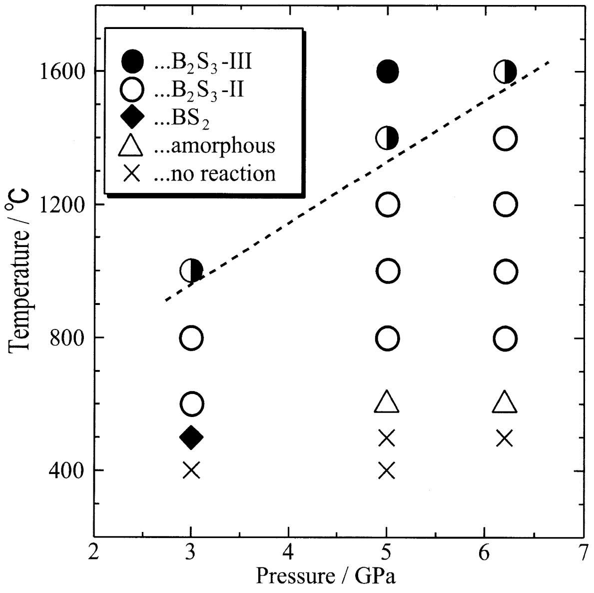

FIG. 2. Pressure–temperature phase diagram for the synthesis of B_2S_3.

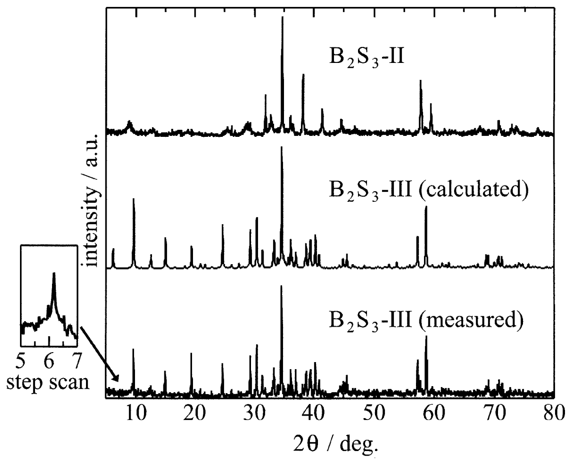

FIG. 3. X-ray diffraction patterns of B_2S_3-II and B_2S_3-III.

B_2S_3-III was obtained at higher temperature region as compared to B_2S_3-II. It appears at 3 GPa and ca. ≥1000°C, and the single phase having pale-yellow color was prepared at 5 GPa and 1600°C. The phase boundary between B_2S_3-II and B_2S_3-III moved to higher temperature with increasing pressure.

Figure 3 shows the X-ray diffraction patterns of B_2S_3-II and B_2S_3-III (additionally, calculated pattern of B_2S_3-III from the structure data analyzed by single crystal). The diffraction pattern of B_2S_3-III consists of sharp reflection peaks only. But that of B_2S_3-II consists of both broad and sharp diffraction peaks. This fact may be one of the reasons why there were no precise reports for high-pressure phases of stoichiometric binary B–S compounds. Moreover, differential thermal analysis could not be performed under high-pressure and temperature conditions due to high vapor pressure of this system. At this stage, B_2S_3-II is anticipated to have a rather disordered structure such as an amorphous material.

The densities of B_2S_3-II and B_2S_3-III were higher than those of any other binary B–S compounds synthesized at ambient pressure. The measured density of B_2S_3-III is 2.48(1) g/cm^3 (the calculated value is 2.479 g/cm^3) while that of B_2S_3 synthesized at ambient pressure is 1.952 g/cm^3 (2). The density of B_2S_3-II is almost the same as B_2S_3-III, suggesting a structural similarity between B_2S_3-II and B_2S_3-III.

At 5 GPa and 1300–1400°C, corresponding to the transition region from B_2S_3-II to B_2S_3-III, tiny crystals of B_2S_3-III having transparent pale-yellow color were frequently obtained. These crystals were grown for single-crystal structure determination by adjusting the heating profile. For the synthesis of powder B_2S_3-III sample, the objective reaction temperature was rapidly achieved within 15–16 min. But for preparing single crystals, the heating rate was kept at 2°C/ min at near the transition region of

B_2S_3-II to B_2S_3-III. This operation was successful to control the nucleation and crystal growth, and to maintain the reaction under high vapor pressure of sulfides carefully.

Crystal Structure of B_2S_3-III

B_2S_3-III consists of B–S bonds only and does not have B–B or S–S bonds. The average B–S bond length is 1.922 Å, in good agreement with that of compounds built up from tetrahedral boron atoms, such as $Na_6B_{10}S_{18}$ (11) and $Li_9B_{19}S_{33}$ (12). The average value of S–B–S bond angles is 109.4°, corresponding to the ideal tetrahedral sp^3-hybridized angle.

B_2S_3-III is made up of nearly regular BS_4-tetrahedra. These tetrahedra constitute two kinds of macrotetrahedra (units 1 and 2) as shown in Fig. 4. Unit 1 consists of 20 BS_4 tetrahedra and has edges composed of four BS_4. Unit 2 consists of 34 BS_4 and has edges composed of five BS_4.

In unit 1, a tetrahedral sulfur atom (S14) resides at the 4*b*-site in the center of the unit. It seems somewhat unstable because the thermal parameters of S14 and the coordinating boron atoms [4(B5)] are relatively larger than those of other atoms, although the values are within a permissible value. This should be due to the mismatch between the actual B–S bond length (1.906 Å) and the ideal bond length deduced from the sum of the tetrahedral radii. In fact, sulfur atoms in other macrotetrahedral compound $Na_6B_{10}S_{18}$ (11) have coordination numbers less than 3. The stabilization of tetrahedral sulfur atom in B_2S_3-III is mainly caused by pressure effect. Such an increase of coordination number is generally observed in many pressure-induced structural transformations. However, there is a possibility of partial deficiency at the S14 site.

As described before, unit 2 has edges composed of five BS_4-tetrahedra, and it could be expected that some tetrahedral sulfur atoms reside in it. But, in fact, a boron atom in the centered position of unit 2 (4*a*-site) is deficient and all sulfur atoms in unit 2 have coordination numbers less than 4.

These units are linked with each other by sharing BS_4-tetrahedra at the corners. Eventually, units 1 and 2 are represented as formulas of $[B_{16}S_{19}\ (4/2)BS_4]^{0\pm} = [B_{18}S_{27}]^{0\pm}$ and $[B_{30}S_{40}\ (4/2)BS_4]^{0\pm} = [B_{32}S_{48}]^{0\pm}$, respectively. On the other hand, macrotetrahedra found in ternary chalcogenides usually have electronic charges i.e., $[B_{10}S_{16}S_{4/2}]^{6-}$ in $Na_6B_{10}S_{18}$ (11) or $[In_{10}S_{18}]^{6-}$ in a recently reported "supertetrahedral" structure with giant cavities and channels (13). Units 1 are tetrahedrally coordinated by four units 2, and units 2 vice versa. Consequently, these units make an infinite three-dimensional network as shown in Fig. 5a. Figure 5b shows the schematic arrangement of these units represented by two kinds of spheres expressing units 1 as small spheres and units 2 as large spheres. Obviously, it can be understood as a zincblende-type connecting network.

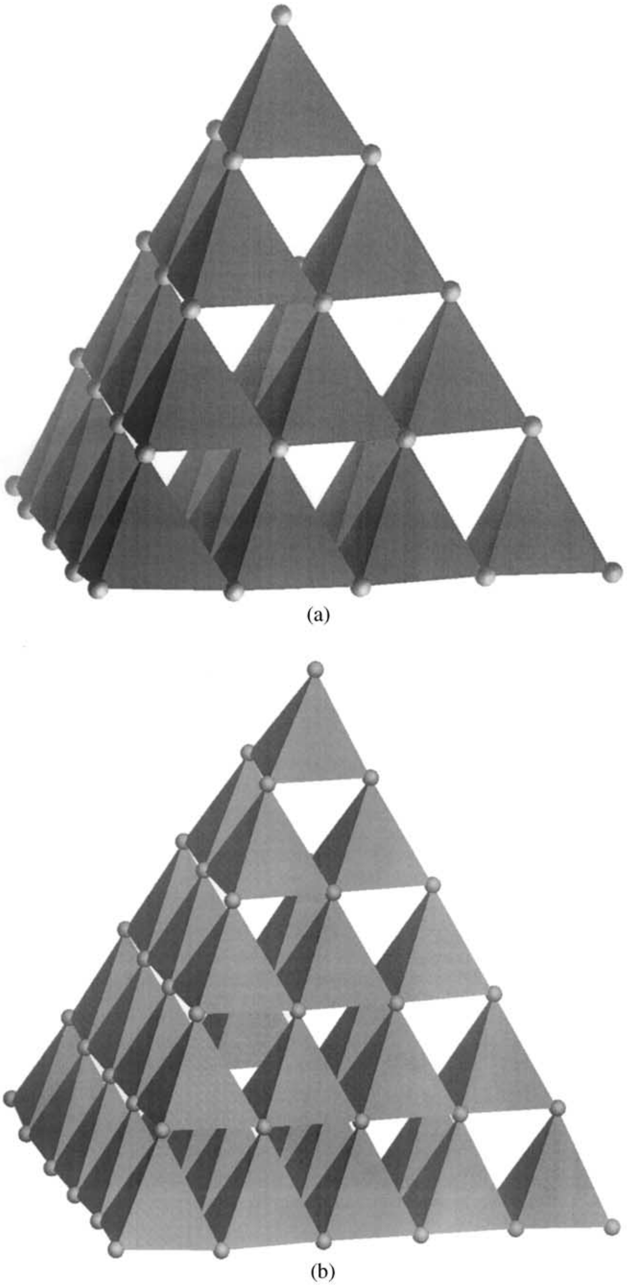
(a)

(b)

FIG. 4. Basic cluster-unit structure in B_2S_3-III: (a) unit 1; (b) unit 2.

In fact, the crystal structure of B_2S_3-III is made up of the interpenetrating networks of this zincblende type as shown in Fig. 6. In other words, it can be mentioned that two zincblende-type networks of macrotetrahedra compose a "double-zincblende superlattice", just like a "double-diamond superlattice" built up from approximately tetrahedral $Cd_{17}S_4(SCH_2CH_2OH)_{26}$ clusters (14).

In the binary B–O system (boron oxide), a pressure-induced phase transition, accompanying the change of coordination number of boron atoms from 3 to 4, is known

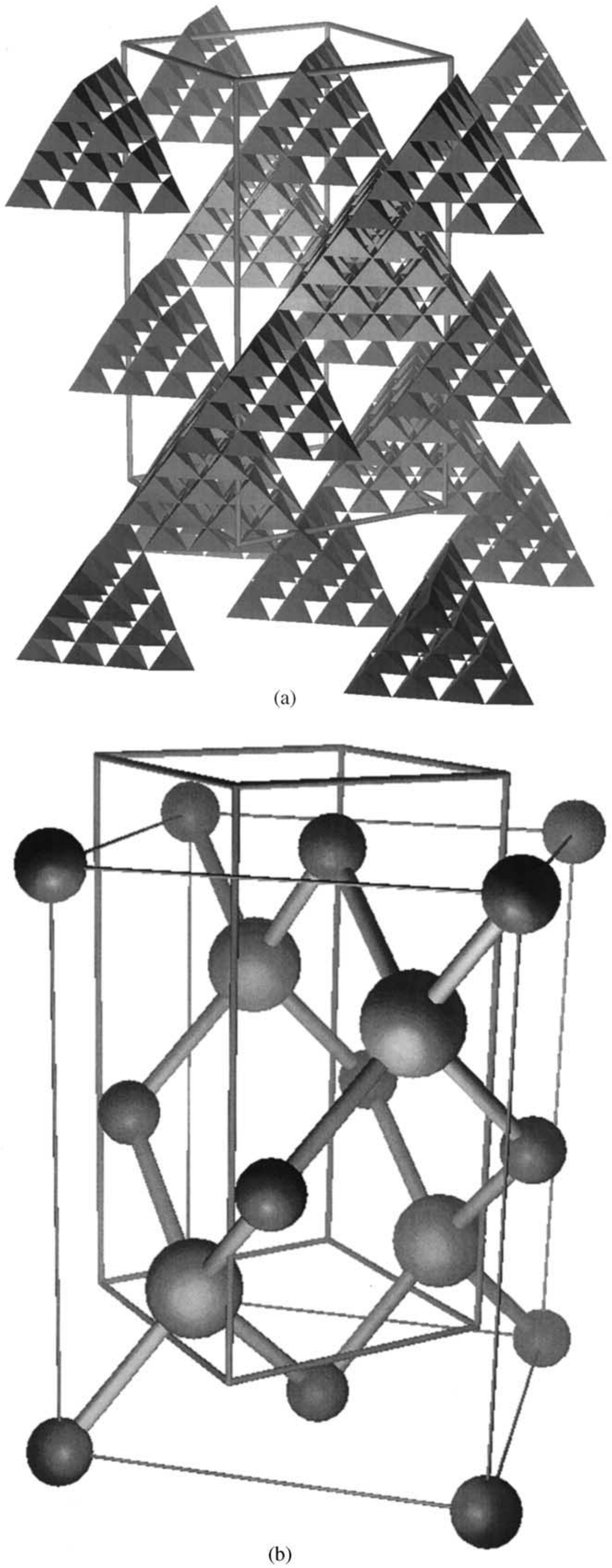

FIG. 5. (a) Arrangement of cluster units (lattice indicates a unit cell). (b) Schematic arrangement of cluster units in B_2S_3-III (smaller spheres indicate unit 1 and others indicate unit 2).

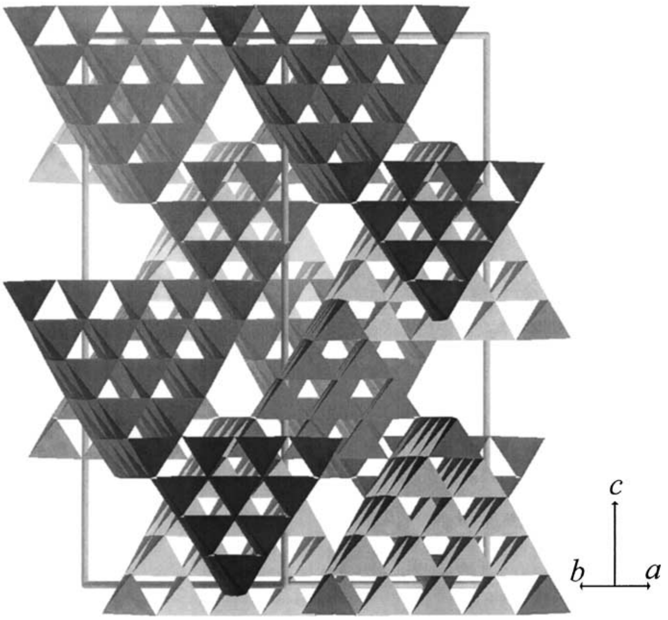

FIG. 6. Crystal structure of B_2S_3-III.

(B_2O_3-I–B_2O_3-II) (15–20). The presence of a similar high-pressure phase transition was predicted in the boron sulfide system before (3), but the determined structure of B_2S_3-III in this study is more complex as compared to B_2O_3-II and other 13_2-16_3-type compounds.

Some Properties of B_2S_3-III

It is known that binary B–S compounds are easily subjected to hydrolysis or oxidation. However, high-pressure phases in this system such as *r*-BS or B_2S_3 (II and III) seem to be more stable than the phases prepared at ambient

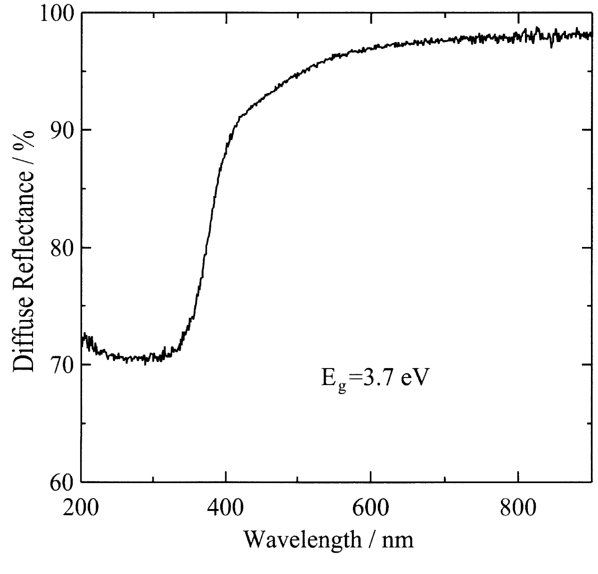

FIG. 7. UV-Vis diffuse reflectance spectrum of B_2S_3-III.

pressure. Nevertheless, these phases are not intrinsically stable and slowly subjected to hydrolysis or oxidation. These aspects were observed from the variation of XRD patterns or infrared absorption spectra of samples kept for a long period at ambient condition.

Figure 7 shows the UV-Vis diffuse reflectance spectrum of B_2S_3-III. It does not show any absorptions in the visible region and the optical band gap was estimated to be 3.7 eV.

CONCLUSIONS

In the present study, two new high-pressure phases of binary B–S system, B_2S_3-II and B_2S_3-III, were synthesized and the structure of B_2S_3-III was determined from the single-crystal diffraction data. B_2S_3-III has a topologically interesting crystal structure built up from two kinds of macrotetrahedra. B_2S_3-II is anticipated having a rather disordered structure.

Regarding the physical properties, the optical band gap of B_2S_3-III was clarified at this stage. The structure and property analyses of high-pressure phases of binary B–S compounds, including B_2S_3-III, are consecutively in progress.

REFERENCES

1. V. I. Matkovich, *J. Am. Chem. Soc.* **83,** 1804 (1961).
2. H. Diercks and B. Krebs, *Angew. Chem. Int. Ed. Engl.* **16,** 313 (1977).
3. B. Krebs, *Angew. Chem. Int. Ed. Engl.* **22,** 113 (1983).
4. B. Krebs and H. U. Hürter, *Angew. Chem. Int. Ed. Engl.* **19,** 481 (1980).
5. H. U. Hürter, B. Krebs, H. Eckert, and W. Müller. Warmuth, *Inorg. Chem.* **24,** 1288 (1985).
6. O. Conrad, C. Jansen, and B. Krebs, *Angew. Chem. Int. Ed.* **37,** 3208 (1998).
7. D. C. Carlson, *Diss. Abstr.* **27,** 2664 (1967).
8. T. Sasaki, H. Takizawa, K. Uheda, and T. Endo, *Phys. Stat. Sol. B* **223,** 29 (2001).
9. SIR92: A. Altomare, G. Cascarano, C. Giacovazzo, A. Guagliardi, M. C. Burla, G. Polidori, and M. Camalli, *J. Appl. Cryst.* **27,** 435 (1994).
10. teXsan: Single Crystal Structure Analysis Software, Version 1.6, Molecular Structure Corporation, The Wood-lands, TX, 1993.
11. A. Hammerschmidt, P. zum Hebel, F. Hiltmann, and B. Krebs, *Z. Anorg. Allg. Chem.* **622,** 76 (1996).
12. F. Hiltmann, P. zum Hebel, A. Hammerschmidt, and B. Krebs, *Z. Anorg. Allg. Chem.* **619,** 293 (1993).
13. H. Li, A. Laine, M. O'Keeffe, and O. M. Yaghi, *Science* **283,** 1145 (1999).
14. T. Vossmeyer, G. Reck, L. Katsikas, E. T. K. Haupt, B. Schulz, and H. Weller, *Science* **267,** 1476 (1995).
15. J. D. Mackenzie and W. F. Claussen, *J. Am. Ceram. Soc.* **44,** 79 (1961).
16. G. E. Gurr, P. W. Montgomery, C. D. Knutson, and B. T. Gorres, *Acta Crystallogr. B* **26,** 906 (1970).
17. S. L. Strong and R. Kaplow, *Acta Crystallogr. B* **24,** 1032 (1968).
18. C. T. Prewitt and R. D. Shannon, *Acta Crystallogr. B* **24,** 869 (1968).
19. A. Takada, C. R. A. Catlow, J. S. Lin, G. D. Price, M. H. Lee, V. Milman, and M. C. Payne, *Phys. Rev. B* **51,** 1447 (1995).
20. Dong Li and W. Y. Ching, *Phys. Rev. B* **54,** 13,616 (1996).